

Free Boundary simulations with the XTOR-2F code

A. Marx, H. Lütjens

*Centre de Physique Théorique, Ecole polytechnique, CNRS, Université Paris-Saclay, F-91128
Palaiseau, France*

Introduction

The XTOR-2F code [1] simulates the 3D dynamics of full bi-fluid MHD instabilities in tokamak plasmas. The initial conditions are given by the CHEASE equilibrium code [2]. A free-boundary version of XTOR-2F has been developed. First, the CHEASE equilibrium, which is limited to closed nested poloidal magnetic flux surfaces, was extended by fitting the magnetic potential at the CHEASE computation domain boundary with a set of external poloidal coils. A thin resistive wall was also added in the computational domain, thus permitting the magnetic field diffusion through the wall. The boundary conditions use Green functions to construct a transfer matrix relating the normal and tangential components of the magnetic field outside the wall with the inside solution. Simulations are shown for axisymmetric vertical instabilities and $n = 1/m = 2$ external kinks, and compared with predictions by large aspect ratio ideal MHD theoretical predictions.

1. Free boundary equilibrium

The CHEASE equilibrium code solves the Grad-Shafranov equation with an infinite conducting wall boundary condition at the plasma surface. To extend it, the virtual casing principle [3] is applied. The currents in a set of poloidal coils are evaluated with toroidal Green functions and are adjusted such that the poloidal magnetic flux ψ_p is constant at the CHEASE plasma boundary. This gives an under-determined linear system solved using Tikhonov regularization $\min(\|Ax - b\|^2 + \|\Gamma x\|^2)$, where Γ is a regularization factor. Fig. 1 shows the poloidal magnetic flux of a free-boundary MHD equilibrium, the thick blue line is the CHEASE equilibrium plasma boundary ψ_p , and the thick red line is the resistive wall. In the following, the zone between ψ_p and the resistive wall will be labeled "SOL", and the one outside the wall "vacuum".

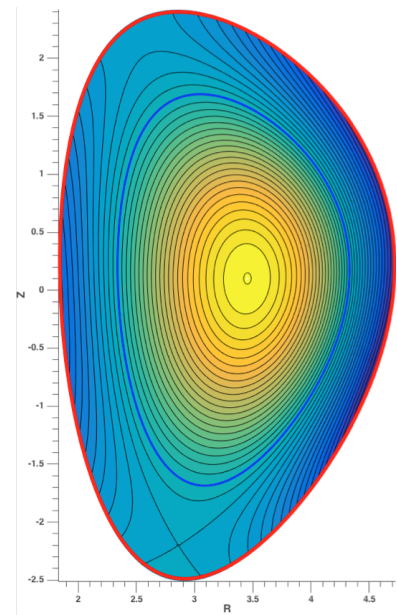


Fig. 1: Poloidal magnetic flux of a free boundary equilibrium extending a CHEASE equilibrium outside ψ_p (blue line).

2. Resistive wall

A thin resistive wall model is used. The magnetic field normal to the wall surface is equal inside and outside the wall, $B_{SOL}^r = B_{vacuum}^r \equiv B_{wall}^r$. The inside component is solution of the full bi-fluid set of equation solved by XTOR-2F. For every toroidal mode number n , the tangential vacuum magnetic field component is linked to the normal one using regularized Green functions by means of a linear system of equations. Here, the corresponding matrices Z^n , are computed with the GRIN code [4].

For a given toroidal mode number $n > 0$, $B_{\theta}^{vacuum} = \partial_{\theta} (Z^n B_r^{wall})$ and $B_{\phi}^{vacuum} = \partial_{\phi} (Z^n B_r^{wall})$. This allows to compute the normal derivatives across the wall, $(\partial_r B_{\theta})_{wall} \sim \frac{B_{\theta}^{vacuum} - B_{\theta}^{SOL}}{\delta_{wall}}$ and $(\partial_r B_{\phi})_{wall} \sim \frac{B_{\phi}^{vacuum} - B_{\phi}^{SOL}}{\delta_{wall}}$, where δ_{wall} is the wall thickness. Therefore, poloidal and toroidal currents in the wall are $j_{wall}^{\theta} = D (\partial_{\phi} B_r - \partial_r B_{\phi})_{wall}$ and $j_{wall}^{\phi} = D (\partial_r B_{\theta} - \partial_{\theta} B_r)_{wall}$, respectively. D is the Jacobian of the XTOR-2F discretization mesh. These currents govern the magnetic field diffusion through the resistive wall, $\partial_t B_{wall}^r = -\eta_w D (\partial_{\theta} j_{\phi} - \partial_{\phi} j_{\theta})$ during the time evolution of the system (η_w is the wall resistivity).

The $n = 0$ mode is handled separately. Instead of the normal magnetic field component B_{wall}^r , the poloidal magnetic flux at the wall ψ is used as variable through $\partial_t \psi = -\eta_w j_{\phi}^{\text{wall}}$. Its normal derivative satisfies $\partial_r \psi = (Z^{n=0})^{-1} \psi$. From which we compute the magnetic field radial and poloidal components $B_{wall}^r = D \partial_{\theta} \psi$ and $B_{vacuum}^{\theta} = -D \partial_r \psi$, respectively. The toroidal component of the magnetic field will evolve independently following $\partial_t B_{wall}^{\phi} = -\eta_w D (\partial_r j_{\theta} - \partial_{\theta} j_r)$.

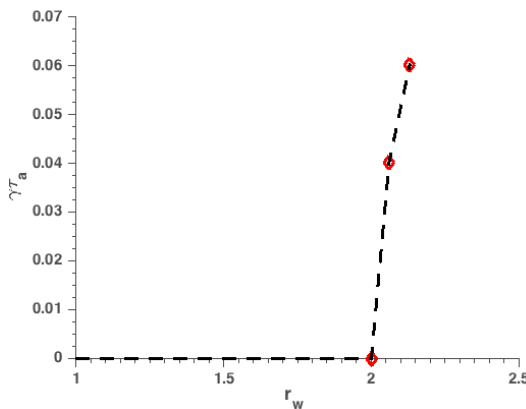


Fig.2.1: Linear growth rate $\gamma\tau_a$ of $n = 0$ axisymmetric mode with perfectly conducting wall boundary conditions versus the wall position r_w for an elongated $\kappa = 1.6$ equilibrium with flat current profile. Symbols are the XTOR-2F simulation results.

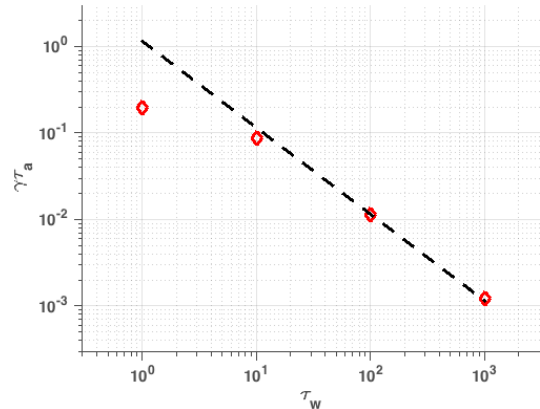


Fig.2.2: Linear growth rate $\gamma\tau_a$ of $n = 0$ axisymmetric mode with resistive wall boundary conditions versus the resistive wall time τ_w . Wall position is set to $r_w = 1.3$. Symbols are the XTOR-2F simulation results. The dashed line is the scaling $\gamma\tau_a = 1/F\tau_w$.

3. Axisymmetric modes

An MHD equilibrium with elongation $\kappa > 1$ triggers an axisymmetric mode instability (i.e. a plasma vertical displacement). This mode can be stabilized by a perfectly conducting wall

sufficiently close to the plasma surface. The criterion for stability is $F = \frac{\kappa+1}{\kappa-1} \left(\frac{1}{r_w} \right)^2 - 1 > 0$, which corresponds to a threshold value for the wall distance of $r_w^c = \sqrt{\frac{\kappa+1}{\kappa-1}}$ [5]. Fig.2.1 shows the linear growth rates of the axisymmetric mode for a flat current profile with $\kappa = 1.6$. The measured threshold is $r_w = 2$, near the theoretical value $r_w^c = 2.08$. In experiments the wall is resistive, an instability will develop even if the wall distance is below the perfectly conducting wall stability threshold $r_w < r_w^c$. Fig.2.2 shows the linear growth rates of the axisymmetric mode with a resistive wall for a flat current profile with $\kappa = 1.6$ and $r_w = 1.3$. The computed growth rate scale with the inverse of the resistive wall time $\gamma\tau_a = 1/F\tau_w$ for large τ_w [6].

4. External Kinks and Resistive Wall Modes (RWM's)

The external kink MHD instability, when studied theoretically in ideal MHD in the large aspect ratio limit, gives the following ODE [7]:

$$\frac{d}{dr} \left\{ r^3 \left(\left(n + \frac{m}{q} \right)^2 - \omega^2 \right) \frac{d\xi}{dr} \right\} - (m^2 - 1) r \left\{ \left(n + \frac{m}{q} \right)^2 - \omega^2 \right\} \xi = 0 \quad (1)$$

with boundary condition $\left(\frac{r\xi'}{\xi} \right)_{r=a} = \left\{ \omega^2 - n^2 + \frac{m^2}{q^2} - \left(n + \frac{m}{q} \right)^2 \mid m \mid \Lambda \right\}$, where $r = a$ is the plasma-SOL interface.

For perfectly conducting and resistive wall boundary conditions, $\Lambda(\tau_w = \infty) = \frac{1 + \left(\frac{a}{b} \right)^{2|m|}}{1 - \left(\frac{a}{b} \right)^{2|m|}}$ and

$\Lambda(\tau_w) = \frac{2|m| - \left(1 + \left(\frac{a}{b} \right)^{-2|m|} \right) i\tau_w \omega}{2|m| - \left(1 - \left(\frac{a}{b} \right)^{-2|m|} \right) i\tau_w \omega}$, respectively, where $\tau_w = \tau_a \delta_w r_w / \eta_w$ is the wall resistive time.

The numerical solution of this ODE gives the instability normal mode ξ for a given q-profile,. The associated eigenvalue is equal to the normalized growth rate $\omega = \gamma\tau_a$. In order to approach this asymptotic model with XTOR-2F, the physical parameters of the simulation need to be fine tuned. The profiles are set constant with a high contrast between the plasma and the SOL for the density ($n_{plasma} = 1$ and $n_{SOL} = 10^{-3}$) and for the Lundquist number ($S_{plasma} = 10^{12}$ and $S_{SOL} = 1$). This is done to approach the ideal MHD behavior in the plasma and a true vacuum in the SOL. The inverse aspect ratio is set to a small value $\epsilon = 0.1$. The wall distance is set to $r_w = 1.2$. The Fig.2 shows good agreement between XTOR-2F simulations (red diamonds) and the above theoretical model (blue line) for the external kinks and RWM's. In Fig.2.1 growth rates are presented in the unstable range of the safety factor $q_a \equiv q_{r=a}$ for the ideal $n = 1/m = 2$ external kink mode. In Fig.2.2, $q_a = 1.6$. In that case, the external kink is stable with a perfectly conducting wall in Fig.2.1 but unstable with a resistive wall. Fig.2.2 shows RWM growth rates as a function of the wall resistive time τ_w for both the theory and the XTOR-2F simulations.

Two regimes are observed: the resistive regime $\tau_w/\tau_a \gg 1$ where the growth rates scale linearly with τ_w and the inertial regime $\tau_w/\tau_a \ll 1$ where the growth rates are constant.

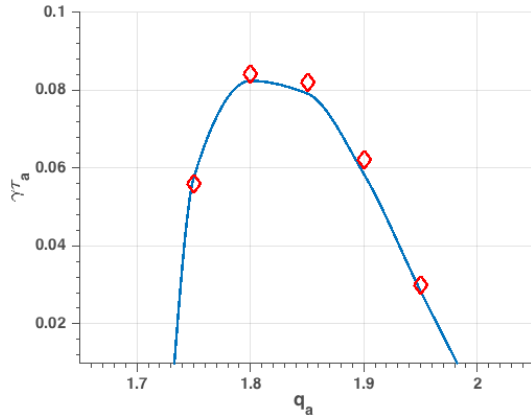


Fig.2.1: Linear growth rate $\gamma\tau_a$ of $n = 1/m = 2$ external kink mode with perfectly conducting wall boundary conditions versus q_a .

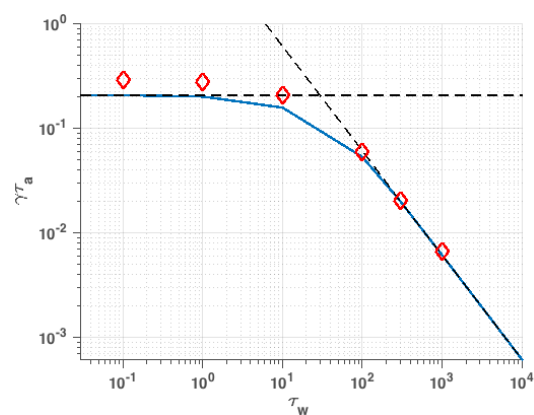


Fig.2.2: Linear growth rate $\gamma\tau_a$ of $n = 1/m = 2$ RWM mode versus the resistive wall time τ_w with $q_a = 1.6$ in Fig.2.1.

Conclusion

A prolongation of CHEASE equilibrium solution to a free boundary equilibrium and a resistive wall boundary condition have been implemented in XTOR-2F extended MHD code. These new equilibrium and boundary conditions have been tested for two external instabilities: the $n = 0$ axisymmetric mode and the $n = 1/m = 2$ external kink and its associated RWM. The linear growth rates are in good agreement with large aspect ratio theoretical results. These results need proper fine tuning of the XTOR-2F simulation parameters in order to approach the asymptotic models hypothesis. This benchmarks the code and allows now to address more complex MHD instabilities. It is planned to investigate active feedback methods on the RWM stability as well as peeling-balloonning modes and disruptions in the near future.

References

- [1] H. Lütjens et al. *Comput. Phys. Comm.* **229** (2010) 8130.
- [2] H. Lütjens, A. Bondeson, and O. Sauter, *Comput. Phys. Comm.* **97** (1996) 219.
- [3] Zakharov, L. E., *Nuclear fusion* **13** (1973) 595.
- [4] A. Pletzer, H.R. Strauss, *Comput. Phys. Comm.* **182** (2011) 2077.
- [5] Laval et al. *Physics of Fluids* **17** (1974) 835.
- [6] Wesson et al. *Nuclear Fusion* **18** (1978) 87.
- [7] Goedbloed et al. *Advanced magnetohydrodynamics*. (Cambridge University Press, 2010)